A Modified Image Processing Algorithm for Error Reduction in Line-of-Sight Vector Between a Spacecraft and Target Celestial Body.

G.K.Rajini[#1], Shaik Naseera[#2], P. Mahalakshmi[#1], Jasmine Pemeena Priyadharshini[#3]
[#1]School of Electrical Engineering, VIT University, Vellore, India.
[#2]School of Computing Science and Engineering, VIT University, Vellore, India.
[#3]School of Electronics Engineering, VIT University, Vellore, India.
[1]rajini.gk@vit.ac.in

Abstract—**Autonomous Navigation is an indispensable technology in which Line-of-Sight (LOS) Vector is very essential. Measuring LOS Vector involves image processing techniques and the existing methodology for this measurement starts with pre-processing of captured raw image of target celestial body. The pre-processing step includes edge detection by Canny Edge Detection Algorithm. Fitzgibbon's Approach to least squares fitting of ellipse is used for fitting the ellipse to the edge data points and to determine the ellipse limb points. With these limb points, ellipse parameters such as ellipse centre, semi-major axis, semi-minor axis, and the inclination angle from the x-axis to the ellipse major axis are computed. Subsequently, the LOS Vector from the spacecraft to the centroid of the target celestial body is obtained. But in this proposed work, a Modified Morphology Based Edge Detection Algorithm is used in the place of Canny Edge Detection Algorithm. Further, the line of sight vector and error in computation is analysed and we noticed that the error is minimized through the proposed method.**

Keyword: Autonomous Navigation, Line-of-Sight Vector, Canny Edge Detection, Modified Morphology, Least Square Ellipse Fitting.

I. INTRODUCTION

Communication link between the satellite and Earth station is made throughout the satellite's working life time. The link is for to-and-fro updates between the Earth-Based Radio Tracking Station(EBRTS) and the satellite. Traditional spacecraft navigation is done by range rate measurements by measuring the parameters like speed, distance and its major drawbacks are high cost and low update frequency. In case of link failure, spacecraft may be lost in space or it may hit any other celestial objects and get destroyed. For manned spacecraft's, even the life of the crew may be crucial [7].Autonomous Navigation helps in preventing these types of hazardous conditions and it is very essential for both robotic and manned deep space exploration missions.The proposed algorithm is more sophisticated,robust and provides minimum error and less computation cost. Autonomous Navigation includes several tasks such as measuring the distance between the spacecraft and the celestial body of its interest, calculating the rotational and revolution speed of the celestial body, and involves successful landing on the surface of the body, continuous observation on the surroundings to avoid collisions etc.The overall assessment of the autonomous navigation system is a separate topic which includes several system dynamics [3]. The multi resolution analysis in wavelets are applied for the characterization of intensity variations in images. Mallat et al shows[1] that the images are approximated by wavelet bases adequately. In noise environment, Canny detector is formulated as an optimization problem [2].

In this paper, A comparative study is made between the Fitzgibbon's approach and improved least square method for fitting ellipse. We have computed the ellipse limb points, ellipse parameters such as ellipse centre, semi-major axis, semi-minor axis, and the inclination angle from the x-axis to the ellipse major axis.

Section 2 gives the related work in the field of study, Section 3 briefs the modified morphological edge detection, section 4 presents the procedure for computation of line of sight vector, Section 5 provides performance measures and Section 6 briefs the results and section 7 presents the conclusions and future enhancements.

II. RELATED WORK

Shuang Li et. al. has depicted the capability of autonomous Optical Navigation (OPNAV) is critical parameter for manned space exploration missions and robotics[10]. To meet the requirements of deep-space autonomous OPNAV, the Least Squares-based ellipse fitting and Levenberg-Marquardt-based ellipse fitting algorithms are developed by them.

A LANDSAT image is chosen and processes to identify the used land[14]. Initially the noise is eliminated in the LANDSAT image and the required features like vegetation indices, used land, forest and unused land are extracted. After extracting the features from the image, classification algorithms like KNN, SVM, Fuzzy algorithms are applied to get the classified image. These results were compared with their modified algorithms like MOKNN and MOSVM and the authors have shown that their modified algorithms gives the better result comparing with the existing algorithms.

Owen [11] has developed a optical navigation method to extract the navigation observables from raw images taken by a spacecraft that includes the line-of-sight vector, angle between horizon and the reference star, apparent diameter and centroid, etc..

Kominato investigated an on-board navigation for Hayabusa employed wide-angle cameras in conjunction with Light Detecting and Ranging (LIDAR) for measurement of altitude with respect to the asteroid Itokawa [12].

ShyamBhaskaran in [13] used an optical-based navigation system to compute line-of-sight vector for the objects that are far-away or closer by.

The optical measurements are the line-of-sight direction vectors from the spacecraft to the landmarks on the surface of the small body with an assumption that the inertial and fixed body locations are known. Authors described in detail about the process of landmark measurements to estimate spacecraft position [12].

We observed that the error rate in computation of observables like centroid, LOS, apparent diameter are more in the mentioned work above. We analysed that morphological approach in combination with Fitzgibbon approach and Improved Least Squares Method provided better results in terms of error rate. This is the motivation factor for us to choose this model in our proposed work.

III. MODIFIED MORPHOLOGY EDGE DETECTION

Morphological edge detection algorithm selects an appropriate structuring element of the processed image and makes use of the basic theory of morphology including erosion, dilation, opening, closing operations, and the synthesization operations. The raw grayscale image of target celestial body is processed using this technique, and the resultant image is shown below. Fig.1 and Fig. 2 represents raw image of planet Mercury taken by Messenger Spacecraft and Gaussian filtered image.

IV. MOFIFIED IMAGE PROCESSING PROCEDURE TO FIND LINE-OF-SIGHT VECTOR

In this work, the image pre-processing technique such as image smootheningis used to suppress the image noise and other small variations inan image. But it blurs the sharp edges, and it is considered as disadvantage, since sharp edges contain valuable information[8].

Fig.1. represents flow chart of modified image processing procedure which involves Gaussian filtering of raw image of a celestial bodyand followed by edge detection through Canny and modified morphological approach. These edges are subjected to Fitzgibbon's approach and improved least square method for fitting ellipse. Next step, involves determination of Centroid and finally Line of Sight Vector is determined.

The objective is to locate a planet or moon in an image with the candidate edge points by which an ellipse must be fitted to these data points. Hough transform provides solution to the problem of ellipse fitting and it is based on clustering and voting techniques. These techniques are robust to noise and require large amounts of memory and computation cost, and proves to be difficult to apply in an on-board computer[4]and this approach was proposed by Fitzgibbon. The method works on segmented data and it is stated to be the first non-iterative ellipse-specific fitting. An ellipse is a special case of a general conic which can be demonstrated by an implicit second order polynomial, Fitzgibbon proposed an appropriate and robust algorithm for an ellipse-specific fitting of data points[6].Improved Least Squares Method for Fitting Ellipses works on segmented data andit is stated to be the first non-iterative ellipse-specificfitting.

V. PARAMETER EXTRACTION

The performance measures of this proposed algorithm based on various parameters like Centroid extraction, Line of Sight Vector and are investigated in the following section.

A. Centroid Extraction

This evaluation approach with centroid extraction produces accurate results in terms of navigation measurements with various parameters, such as the shadows in an image of a planet which depends on the illumination and observation angles, and the interference of craters, texture, andatmosphere when photographed from a close range.The centre of an ellipse can be obtained by the transformation from the implicitcoefficients to standard ellipse parameters, which is a well-known result from classicalgeometry, with this evaluation parameters computationof line-of-sight vector from the spacecraft to the centroid of a target celestial body is achieved. Compared with a method directly extracting the centre-of-brightness (COB), the centroid approach achieves a better accuracy of navigation measurements with various influences, such as the shadows in an image of a planet which depend on the illumination and observation angles, and the interference of craters, texture, andatmosphere when photographed from a closer range.

B. Line-Of-Sight Vector Measurement

Once ellipse parameters like co-ordinates of the ellipse center, semi-major axis, semi-minor axis and the inclined angle from the x-axis to the ellipse major axis are found, Line-of-Sight Vector can be computed using some geometric relations [5]. It is already discussed that the co-ordinates of ellipse center is considered as the centroid of the ellipse and is shown in Fig. 5.

The line of Sight vector is rotated from the camera frame to the inertial frame,

$$e_i^I = T_B^I . T_C^B . e_i^C \tag{1}$$

where T_B^I is the transformation matrix from body frame to inertial frame, T_C^B is the transformation matrix from camera frame to body frame.

As it is already known that,

$$T_B^I . T_C^B = T_C^I \tag{2}$$

Therefore equation (8) becomes,

$$e_i^I = T_C^I . e_i^C \tag{3}$$

where T_C^I is the transformation matrix from camera frame to inertial frame and,

$$T_C^I = \begin{bmatrix} 1 & 0 & 0 \\ 0 & 0 & -1 \\ 0 & 1 & 0 \end{bmatrix} \tag{4}$$

With the help of equation (10), Line-of-Sight Vector is measured. But the actual center of the target celestial body is given as the intersection point of horizontal and vertical axis on the captured raw image. It is given that the centroid as (half of the column size, half of the row size). Let the column size be 'n' and row size as 'm'. The actual centroid is given as (5),

$$(u_j, v_j) = (\frac{n}{2}, \frac{m}{2})$$

The next step is to find the error in LOS Vector. The error is calculated between the measured LOS Vector and the actual LOS Vector. Let the measured LOS Vector be $e_i^I = (u_{xi}, u_{yi}, u_{zi})$ and the actual LOS Vector be $e_j^I = (u_{xj}, u_{yj}, u_{zj})$. The angle between e_i^I and e_j^I is to be calculated using the dot product between the two. The angle and the error in LOS Vector is related as, the error in LOS Vector is less, if the angle between the two LOS Vectors is less. It is directly related. To find the angle between the two vectors, cosine angle is to be used as,

$$Cos\, \Theta = \frac{(e_i^I . e_j^I)}{(|| e_i^I || . || e_j^I ||)} \tag{5}$$

$|| e_i^I ||$ is the length of the vector e_i^I, $|| e_j^I ||$ is the length of the vector $|| e_j^I ||$, and $(e_i^I . e_j^I)$ is the scalar product of the two vectors.

$$(e_i^I . e_j^I) = (u_{x_i} . u_{x_j}) + (u_{y_i} . u_{y_j}) + (u_{z_i} . u_{z_j}) \tag{6}$$

$$|| e_i^I || = \sqrt{((u_{x_i}{}^2) + (u_{y_i}{}^2) + (u_{z_i}{}^2))} \tag{7}$$

$$|| e_j^I || = \sqrt{((u_{x_j}{}^2) + (u_{y_j}{}^2) + (u_{z_j}{}^2))} \tag{8}$$

By using equations (12) – (15), error in LOS Vector, Θ can be calculated, and it is in radians.

VI. NUMERICAL RESULTS AND ANALYSIS

To test the performance of this algorithm,real images obtained from deep-space flight missions are utilized to realize its robustness and effectiveness. Three raw images captured by different spacecraft's are taken for study. The methodology is applied to all these raw images and the simulation results are mentioned in the tabular columns with their corresponding images. At first, Mercury image captured by Messenger spacecraft is taken for study. The existing and the proposed image processing algorithm are applied to it. The size of the raw image is 2025*3000 pixels. The execution time is 224.15 seconds since the image resolution is very high. The Fig. 6 to Fig. 9 given in Table 1 shows the process of the modified image processing algorithm which involves Canny and modified morphological approach followed by Least square fitting of ellipse.

Fitzgibbon Least Square Fitting of Ellipse for Canny Edge Detection (FLSF – C), Fitzgibbon Least Square Fitting of Ellipse for Modified Morphology Edge Detection (FLSF – MM), Improved Least Square Fitting of Ellipse for Canny Edge Detection (ILSF – C), Improved Least Square Fitting of Ellipse for Modified Morphology Edge Detection (ILSF – MM) observed for different coordinates of the planets Mercury, Venus and Moon are shown in Table 2 to Table 4. Table 2 shows the deputed center coordinate, semi major axis, semi-minor axis, inclined angle, LOS vector and Error in Loss vector for the planet Mercury.

TABLE I. REDUCTION IN LOS VECTOR ERROR FOR THE PLANET MERCURY TAKEN BY MESSENGER SPACECRAFT

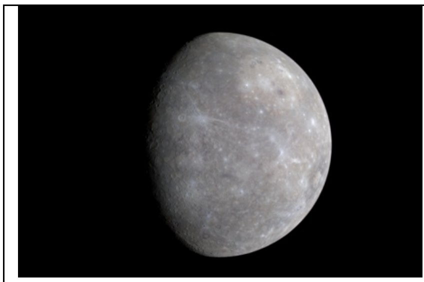	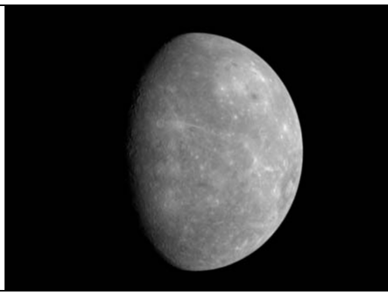	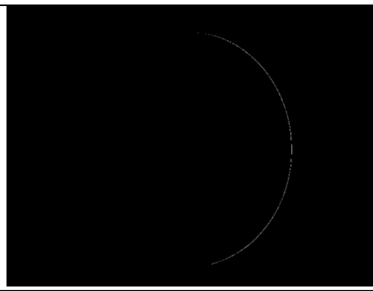
Fig. 1. Raw Image of Planet Mercury taken by Messenger Spacecraft	Fig. 2. Gaussian Filtered Image	Fig. 3. Modified Morphology Method of Edge Detection

From Table 1, it is observed that there is a reduction in LOS Vector error for Modified Morphology edge detection approach than in canny edge detection approach, since the reduction in angle between the vectors.

TABLE II. COORDINATES FOR PLANET MERCURY

Methodology	Center Coordinate	Semi Major Axis a	Semi Minor Axis b	Inclined Angle (radians)	LOS Vector	Error in LOS Vector (radians)
FLSF – C	(1489,994)	838.5343	838.0899	-0.1287	-0.8266; -0.1110; -0.5518	0.0052
FLSF – MM	(1486.2,993.13)	839.6094	840.7927	0.0293	-0.8263; -0.1112; -0.5522	0.0048
ILSF – C	(1489,994)	838.5343	838.0899	-0.1287	-0.8266; -0.1110; -0.5518	0.0052
ILSF – MM	(1486.2,993.13)	847.927	839.6094	1.6001	-0.8263; -0.1112; -0.5522	0.0048

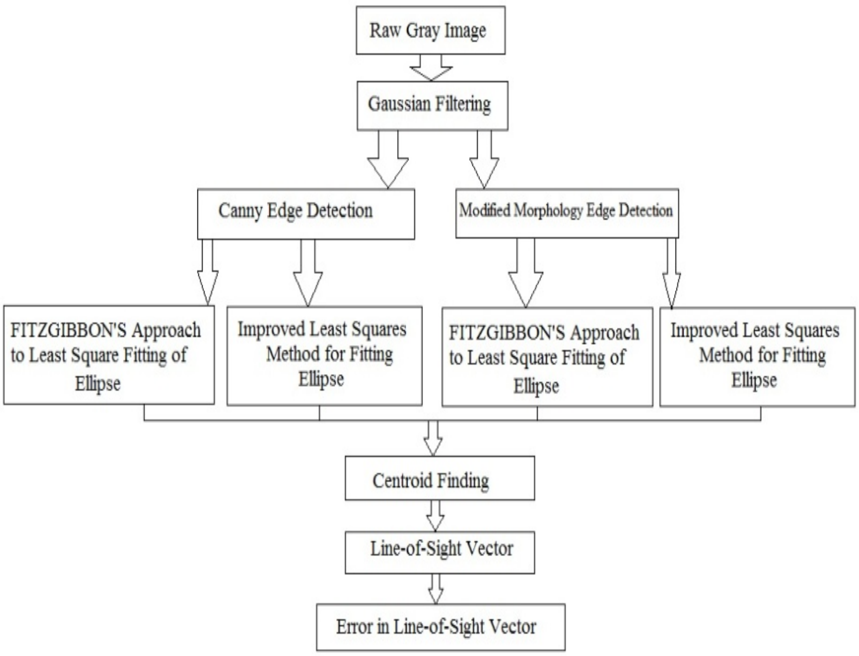

Fig.4. Sketch of Modified Image Processing Procedure to find Line-of-Sight Vector

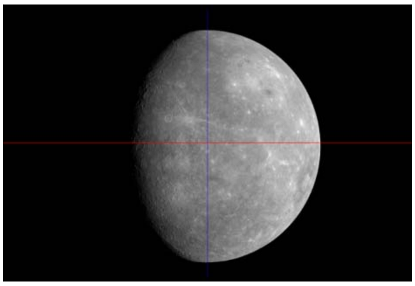

Fig. 5. Intersection of horizontal and vertical axis – actual Centroid finding

Secondly, Venus image captured by Messenger spacecraft is taken for discussion. The size of the raw image is 3456*3428 pixels. The execution time is 410.816 seconds since the image resolution is very high and the results are represented in the Fig.10 to Fig. 17. Table 3 shows the deputed center coordinate, semi major axis, semi-minor axis, inclined angle, LOS vector and Error in Loss vector for the planet Venus.

Fig 6. Fitzgibbon Least Square Fitting of Ellipse - Canny Approach

Fig 7. Fitzgibbon Least Square Fitting of Ellipse –Modified Morphology Approach

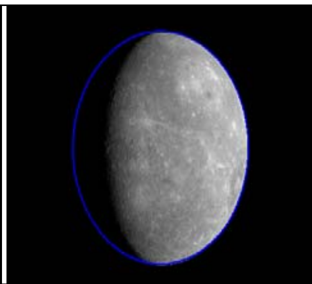

Fig 8. Improved Least Square Fitting of Ellipse – Canny Approach

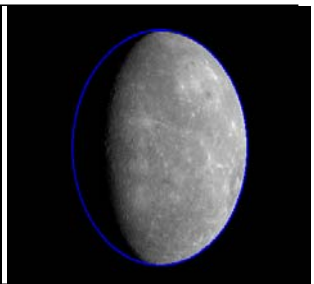

Fig 9. Improved Least Square Fitting of Ellipse –Modified Morphology Approach

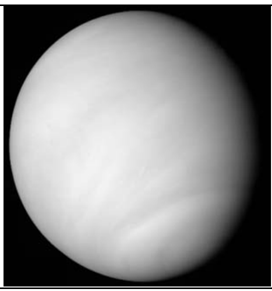

Fig. 10. True image of Planet Venus taken by Messenger Spacecraft

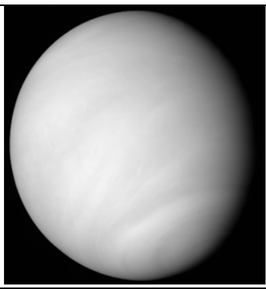

Fig. 11. Gaussian Filtered Image – Planet Venus

Fig. 12. Canny Edge Detected Image – Planet Venus

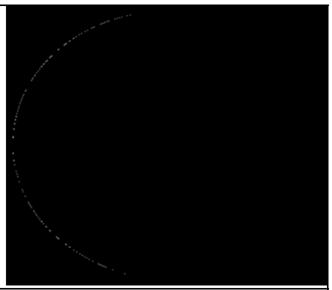

Fig. 13. Edge Detected Image using Modified Morphology Approach – Planet Venus

Fig. 14. Fitzgibbon Least Square Fitting of Ellipse – Canny Approach – Planet Venus

Fig. 15. Fitzgibbon Least Square Fitting of Ellipse – Modified Morphology Approach – Planet Venus

Fig. 16. Improved Least Square Fitting of Ellipse – Canny Approach – Planet Venus

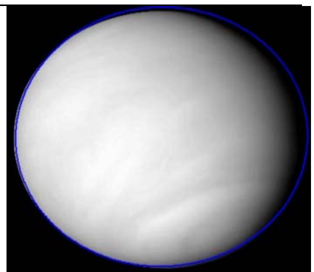

Fig. 17. Improved Least Square Fitting of Ellipse –Modified Morphology Approach – Planet Venus

Fig. 18. True image of Moon obtained from NASA Database

Fig. 19. Gaussian Filtered Image – The Moon

Fig. 20. Canny Edge Detected Image – The Moon

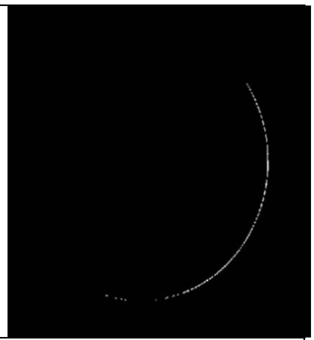

Fig. 21. Edge Detected Image using Modified Morphology Approach – The Moon

Fig. 22. Fitzgibbon Least Square Fitting of Ellipse – Canny Approach – The Moon

Fig. 23. Fitzgibbon Least Square Fitting of Ellipse – Modified Morphology Approach – The Moon

Fig. 24. Improved Least Square Fitting of Ellipse – Canny Approach – The Moon

Fig. 25. Improved Least Square Fitting of Ellipse –Modified Morphology Approach – The Moon

TABLE III. REDUCTION IN LOS VECTOR ERROR FOR THE PLANET VENUS TAKEN BY MESSENGER SPACECRAFT

Methodology	Center Coordinate	Semi Major Axis a	Semi Minor Axis b	Inclined Angle (radians)	LOS Vector	Error in LOS Vector (radians)
FLSF – C	(1702,1755.4)	1617.7	1608.2	1.9621	-0.6938; -0.0815; -0.7156	0.0114
FLSF – MM	(1748.5,1762.8)	1662.4	1632.1	-0.3096	-0.7019; -0.0803; -0.7077	0.0016
ILSF – C	(1702,1755.4)	1617.2	1608.7	0.3913	-0.6938; -0.0815; -0.7156	0.0114
ILSF – MM	(1748.5,1762.8)	1662.1	1632.4	1.2612	-0.7019; -0.0803; -0.7077	0.0016

TABLE IV. REDUCTION IN LOS VECTOR ERROR FOR THE MOON OBTAINED FROM NASA DATABASE

Methodology	Center Coordinate	Semi Major Axis a	Semi Minor Axis b	Inclined Angle (radians)	LOS Vector	Error in LOS Vector (radians)
FLSF – C	(252.6470,313.7288)	242.5328	240.1712	1.2922	-0.5618; -0.4447; -0.6976	0.0950
FLSF – MM	(252.6807,313.5450)	241.9875	240.0791	1.2284	-0.5620; -0.4448; -0.6974	0.0947
ILSF – C	(252.6470,313.7288)	242.5328	240.1712	2.8630	-0.5618; -0.4447; -0.6976	0.0950
ILSF – MM	(252.6807,313.5450)	241.9875	240.0791	2.7992	-0.5620; -0.4448; -0.6974	0.0947

Third, Moon image obtained from NASA Database is taken for study. The size of the raw image is 579*577 pixels. The execution time is 11.15 seconds since the image resolution is very low and the results are represented in Fig. 18 to Fig. 25. In Table 4, presents the center coordinate, semi major axis, semi-minor axis, inclined angle, LOS vector and Error in Loss vector for the planet Moon.

It is observed that the error in computation of Line of Sight Vector is less when the simulation is performed for the planets Mercury, Venus, and Moon in our proposed algorithm. It is further observed that Modified Morphological approach outperforms the conventional edge detection technique with the combination of Fitzgibbon Least Squares-based ellipse fitting and improved Least Square-based ellipse fitting algorithms in terms of error reduction.

VII. CONCLUSION AND FUTURE SCOPE

The capability of autonomous navigation is critical for robotics and manned deep-space exploration missions. New image processing algorithms, Modified Morphology Based Edge Detection are proposed and Fitzgibbon Least Squares-based ellipse fitting and Improved Least Square-based ellipse fitting algorithms, are involved in this proposed work to meet the requirements of deep-space autonomous navigation. Flight images from the MESSENGER mission and NASA Database are utilized to interpret the developed algorithm in this work. Numerical results predicts that combined methods proposed can accurately extract the navigation observables from the raw images. But in particular, Modified Morphology based edge detection with Improved Least Square based ellipse fitting gives better performance. The error of the line-of-sight vector to the object centre is less than 0.001 radians, which can satisfy the requirements of deep-space autonomous navigation.

Future work will be focussed on decreasing the error in LOS Vector by using Levenberg Marquardt based ellipse fitting and end-to-end assessment of the results of a complete autonomous navigation algorithm.

REFERENCES

[1] Mallat S. Zero-crossings of a wavelet transform. IEEE Trans. Inform. Technol. IT-37, 1991, 1019–1033.

[2] Canny J. A Computational Approach to Edge Detection. IEEE Transactions on Pattern Analysis and Machine Intelligence. 1986, 8(6) 697-698.

[3] Christian JA, Lightsey EG. Onboard Image Processing Algorithm for a Spacecraft Optical Navigation Sensor System. Journal of Spacecrafts and Rockets. 2012, 49(2) 337-352.

[4] Fitzgibbon, Andrew. Direct Least Square Fitting of Ellipses. Pattern Analysis and Machine Intelligence. 1999, 21(5) 476-480.

[5] Gonzalez, Rafael C Woods, Richard E. Digital Image Processing, Prentice Hall: USA. 2006.

[6] Halir, Radim, Flusser. Numerically Stable Direct Least Squares Fitting of Ellipses, International Conferences in Central Europe on Computer Graphics, Visualization and Computer Vision, Czech Republic. 1998, Vol. 3, pp. 43-50.

[7] Owen Jr, William M. Methods of Optical Navigation. Advances in the Astronautical Sciences, 2011. 140 1635-1653.

[8] Shuang Li, Ruikun Lu. Image Processing Algorithms for Deep-Space Autonomous Optical Navigation. The Journal of Navigation. 2013, 66(4) 605-623.

[9] Vijaya Kishore V, Satya Narayana RVS. A Modified Mathematical Morphology based approach for Medical Image Edge Detection and Restoration. IUP Journal of Electrical and Electronics Engineering. 2012, V(2) 73-80.

[10] Li S, Lu R, Zhang L, Peng Y. Image processing algorithms for deep-space autonomous optical navigation. J. Navig. 2013, 66, 605–623.

[11] Owen Jr, William M, Philip JD, Coralie DJ. Optical Navigation Preparations For New Horizons Pluto Flyby.

[12] Bhaskaran S, Nandi S, Broschart S, Wallace M, Cangahuala L, Olson C. Small Body Landings Using Autonomous Onboard Optical Navigation. The Journal of the Astronautical Sciences. 2011, 58(3), 409–427.

[13] Bhaskaran S. Autonomous Navigation for Deep Space Missions. SpaceOps 2012 Conference, 2012.

[14] Kumar N. Suresh, Arun M. Enhanced Classification Algorithms for the Satellite Image Processing. Indian Journal of Science and Technology 8.15 (2015).